Available online at www.sciencedirect.com
SCIENCE DIRECT®
Bioorganic & Medicinal Chemistry 13 (2005) 2981–2991
Bioorganic & Medicinal Chemistry

Investigations of linker structure on the potency of a series of bidentate protein tyrosine phosphatase inhibitors

Jian Xie and Christopher T. Seto*

Department of Chemistry, Brown University, 324 Brook St. Box H, Providence, RI 02912, United States

Received 20 December 2004; revised 1 February 2005; accepted 1 February 2005

Abstract—Protein tyrosine phosphatases (PTPases) and protein tyrosine kinase (PTKases) regulate the phosphorylation and dephosphorylation of tyrosine residues in proteins, events that are essential for a variety of cellular functions. PTPases such as PTP1B and the *Yersinia* PTPase play an important role in diseases including type II diabetes and bubonic plague. A library of 67 bidentate PTPase inhibitors that are based on the α-ketocarboxylic acid motif has been synthesized using parallel solution-phase methods. Two aryl α-ketocarboxylic acids were tethered to a variety of different diamine linkers through amide bonds. The compounds were assayed in crude form against the *Yersinia* PTPase, PTP1B, and TCPTP. Six compounds were selected for further evaluation, in purified form, against the *Yersinia* PTPase, PTP1B, TCPTP, LAR, and CD45. These compounds had IC_{50} values in the low micromolar range against the *Yersinia* PTPase, PTP1B, and TCPTP, showed good selectivity for PTP1B over LAR, and modest selectivity over CD45. The correlation between linker structure and inhibitor activity shows that aromatic groups in the linker can play an important role in determining binding affinity in this class of inhibitors.

1. Introduction

One of the central mechanisms by which intracellular signal transduction pathways are regulated relies on the phosphorylation state of specific tyrosine residues in signaling proteins. Control is mediated by protein tyrosine kinases (PTKs) that phosphorylate tyrosine residues, and protein tyrosine phosphatases (PTPases) that dephosphorylate phosphotyrosine residues. The balanced activity of the PTKs and PTPases is critical for controlling a wide variety of cellular functions such as cell growth, intercellular communication, migration, metabolism, gene transcription, and the immune response.[1]

Deregulation of PTPase activity can play a role in a number of diseases including diabetes, cancer, and dysfunction of the immune system. For example, overexpression of PTP1B has been implicated in the development of type II diabetes because this PTPase dephosphorylates the insulin receptor and causes resistance to insulin.[2] PTP1B is now commonly accepted as a valid target for the treatment of type II diabetes, and perhaps obesity, because a PTP1B knockout mouse was shown to have an increased sensitivity to insulin and was resistant to diet-induced obesity.[3,4]

Other PTPases are more complicated in their biological activities. T-Cell protein tyrosine phosphatase (TCPTP), which is the PTPase that is most closely related to PTP1B, is vital in terms of its biological functions. TCPTP knockout mice die at 3–5 weeks of development.[5] However, this PTPase might be useful as a target for the treatment of colon cancer since it has been reported that 70% of 14 colon cancer cases in one study showed an increased activity of TCPTP.[6]

Like PTP1B, leukocyte antigen related PTPase (LAR) is also a negative regulator of the insulin signaling pathway. However, LAR-deficient mice have shown neuronal defects, impaired development of mammary glands, and reduced weight.[7–9] There is one report that increased expression levels of LAR can suppress the formation of tumors in vivo.[10] CD45 is a receptor type PTPase that regulates the activity of the Src-family of kinases. This PTPase is required for normal development and activation of B and T cells,[11] and humans who are deficient in CD45 have impaired immune systems.[12] Inhibitors for this PTPase may be useful for

Keywords: Divalent inhibitor; Phosphatase; Linker; α-Ketocarboxylic acid.
* Corresponding author. Tel.: +1 401 863 3587; fax: +1 401 863 9368; e-mail: christopher_seto@brown.edu

0968-0896/$ - see front matter © 2005 Elsevier Ltd. All rights reserved.
doi:10.1016/j.bmc.2005.02.001

conditions that are related to the immune response including inflammation, organ transplantation, and autoimmune diseases.[13,14] The bacterial PTPase from *Yersinia pestis*, which is the causative agent of bubonic plague, plays a key role in the virulence of this organism. The bacterium secretes the *Yersinia* PTPase (YopH) into host cells, where it dephosphorylates a number of signaling proteins and results in an weakened immune response.[15] All of these studies suggest that selective PTPase inhibitors would be useful as starting points for drug development aimed at a variety of diseases, and also as tools for unraveling the details of signal transduction.

A large number of PTPase inhibitors have reported to date, a small sampling of which include difluoromethylenesulfonic acids,[16] *O*-carboxylmethyl salicylic acids,[17] squaric acids,[18] and α-ketocarboxylic acids.[19–22] These functional groups act as nonhydrolysable mimics of phosphotyrosine, and bind in the active site proximal to the catalytic residues. The catalytic domain of PTPases contains the signature motif (H/V)**C**X_5**R**(S/T), which is highly conserved in all members of this enzyme family.[23] High homology in the catalytic domain of PTPases makes it a significant challenge to develop selective inhibitors.

In 1997, Zhang and co-workers discovered a secondary binding site in PTP1B that is distal from the catalytic site, and that has a lower affinity for phosphotyrosine.[24] This secondary site is made up of residues that include Arg-24, Arg-254, Gly-259, Gln-262, and Met-258 (PTP1B numbering). Amino acid sequence alignment shows that Arg-24 is conserved in PTP1B, TCPTP, and the *Yersinia* PTPase, but not in LAR and CD45. Moreover, Gly-259 and Met-258 are less conserved in PTPases than the residues found in the active site. Based upon their discovery of this secondary binding site, Zhang and co-workers suggested a strategy for designing more potent and specific inhibitors that involves linking together two phosphotyrosine mimics, one of which is targeted to the active site, and the other targeted to the secondary binding site.[1,24] This strategy has been applied successfully by a number of investigators. For example, a group from Abbott Laboratories used NMR-based screening methods to discover two different ligands that bind in the active site and the secondary site, respectively. They then connected these two ligands together with an appropriate linker to generate an oxalylamide-based inhibitor that showed low nanomolar activity against PTP1B and TCPTP, with good selectivity over LAR and CD45. A crystal structure of the inhibitor bound in the active site proved that it made important contacts with both the active site and the secondary binding site.[25] Several other groups have also reported bidentate inhibitors that show significantly improved potency and selectivity when compared to the related monomeric inhibitors.[20,22,26–28] In several cases, structural studies have shown that some of these bidentate inhibitors make contacts with the active site and residues such as Arg-47, Asp-48, and Lys-41, rather than bridging the active and secondary binding sites.[20,22,29–31]

We have recently reported that aryl α-ketocarboxylic acids such as compound **1** are competitive inhibitors of several PTPases.[19] The potency of the inhibitors can be improved by adding electron donating groups to the *para* position of the aromatic ring, and linking two α-ketocarboxylic acids together to give bivalent inhibitors.[20] In this study, we are interested in investigating how the structure and conformation of a linker that connects two α-ketocarboxylic acids influences the potency of inhibition. To accomplish this goal, we have constructed a 69-membered library of divalent inhibitors with the general structure **2**. The aryl α-ketocarboxylic acid portions of the inhibitors remain constant, while changes are made to the linker region that connects them. The inhibitors were assayed in crude form against the *Yersinia* PTPase, PTP1B, and TCPTP, and six compounds were selected for purification and further evaluation.

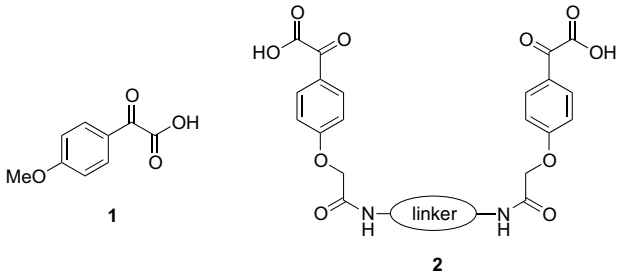

2. Chemistry

The strategy that we employed for assembling the library of divalent inhibitors is shown in Scheme 1. Two equivalents of compound **3**, which incorporates a *tert*-butyl ester of the α-ketocarboxylic acid moiety, was coupled with one equivalent of a number of different diamines using EDC and DMAP to give the diamide **4**. The *tert*-butyl ester groups were then removed with TFA to give the desired inhibitors **2**.

The synthesis of compound **3** is outlined in Scheme 2. 4′-Hydroxyacetophenone **5** was converted to compound **6** using a Williamson ether synthesis with benzyl bromoacetate and potassium carbonate.[32] Oxidation of the methylketone to the α-ketocarboxylic acid was

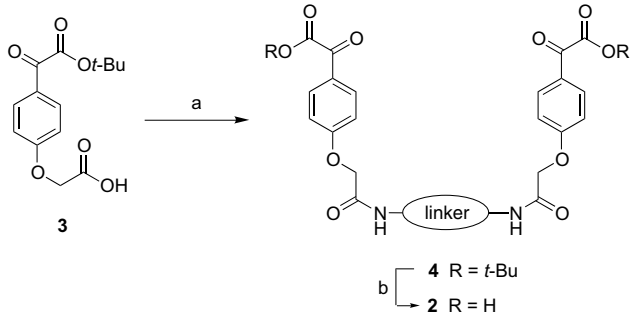

Scheme 1. Reagents: (a) diamine, EDC, DMAP, CH_2Cl_2; (b) TFA, CH_2Cl_2.

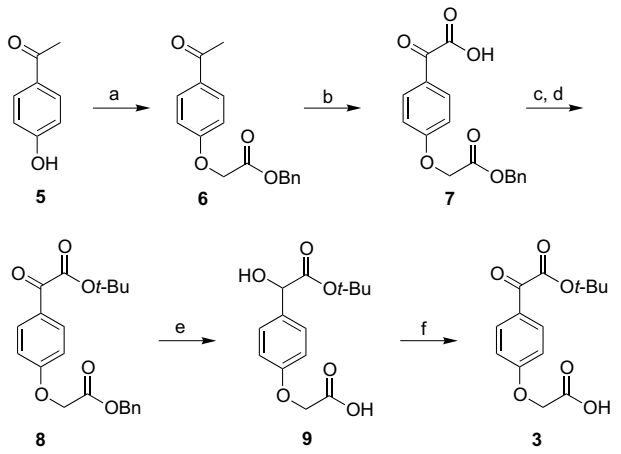

Scheme 2. Reagents: (a) benzyl bromoacetate, K_2CO_3, DMF; (b) SeO_2, pyridine, reflux; (c) $SOCl_2$, benzene, reflux; (d) *t*-BuOH, pyridine, CH_2Cl_2; (e) H_2, $Pd(OH)_2$, EtOAc; (f) Dess–Martin periodinane, acetone.

accomplished using selenium dioxide in refluxing pyridine.[33] The crude product **7** from this oxidation was directly converted to the corresponding acid chloride, and subsequently treated with *tert*-butanol and pyridine to give *tert*-butyl ester **8**. The overall yield for the three step sequence was 71%. The benzyl ester was then deprotected by catalytic hydrogenation using palladium hydroxide. This transformation was accompanied by reduction of the ketone to the corresponding α-hydroxy-ester **9**. The hydroxyl group was oxidized back to the α-ketoester using Dess–Martin periodinane to yield the desired compound **3**.

With compound **3** in hand, we synthesized the library by coupling **3** with the 68 diamines shown in Figure 1. We also coupled compound **3** to aniline (**D1**), benzyl alcohol (**D2**), and 1,2-bis(hydroxymethyl)benzene (**D14**) to give three control compounds for comparison with the diamide-based inhibitors. After the coupling reactions were judged to be complete by TLC analysis, an aqueous workup was used to remove EDU, DMAP, and any excess starting materials. The coupling products were then deprotected using 80% TFA in CH_2Cl_2 to yield the final crude inhibitors. ESI-LCMS was used to confirm the success of the coupling and deprotection reactions. After biological evaluation of the crude inhibitors, six compounds (compounds **11**, **13**, **15**, **17**, **19**, and **21**, corresponding to diamines **D52**–**D54**, **D62**, **D70**, and **D71**)

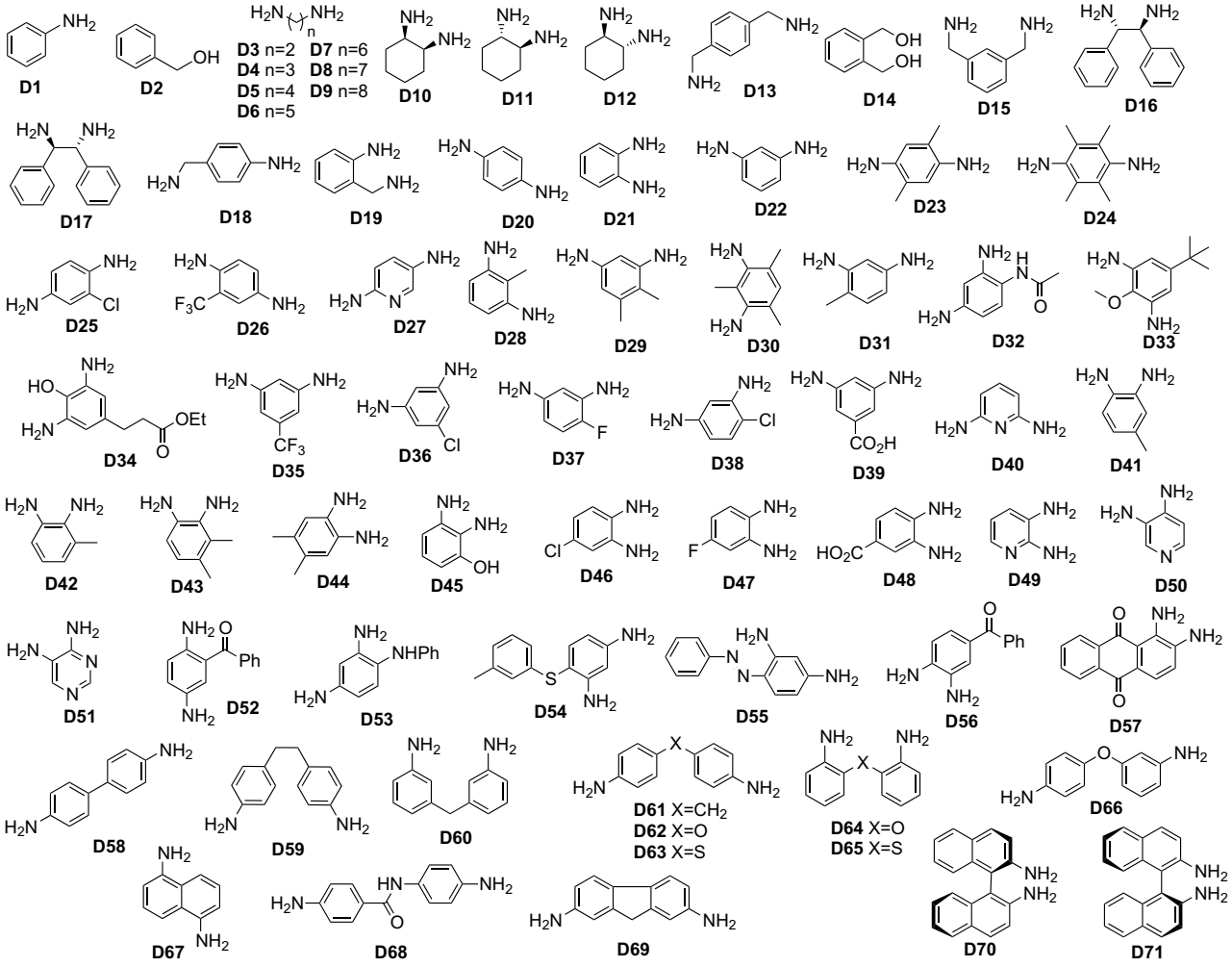

Figure 1. Linkers used to synthesize the library.

were selected for resynthesis on a larger scale (Fig. 2). These six compounds were purified by flash chromatography prior to their further evaluation against a battery of phosphatases.

While the large majority of the diamines shown in Figure 1 resulted in the desired bivalent ligands, several of the reactions gave unexpected products. For example, diamine **D53** has two primary and one secondary amino groups that could potentially couple to carboxylic acid **3**. However, based upon both steric and electronic considerations, we expected only the primary amino groups to react with compound **3** under our coupling conditions to give diamide **12** (Fig. 2). As expected, compound **12** was the only product that we observed from the coupling reaction. However, when compound **12** was treated with TFA to remove the *tert*-butyl esters, the molecule gave the cyclic compound **13** in which one of the α-ketocarboxylic acid groups had spontaneously formed a third amide linkage with the secondary amine. Since this macrocyclic compound showed good activity in our preliminary screens, we selected it for purification and further evaluation.

The coupling reaction between diamine **D54** and compound **3** gave mono-amide **14** as the only detectable

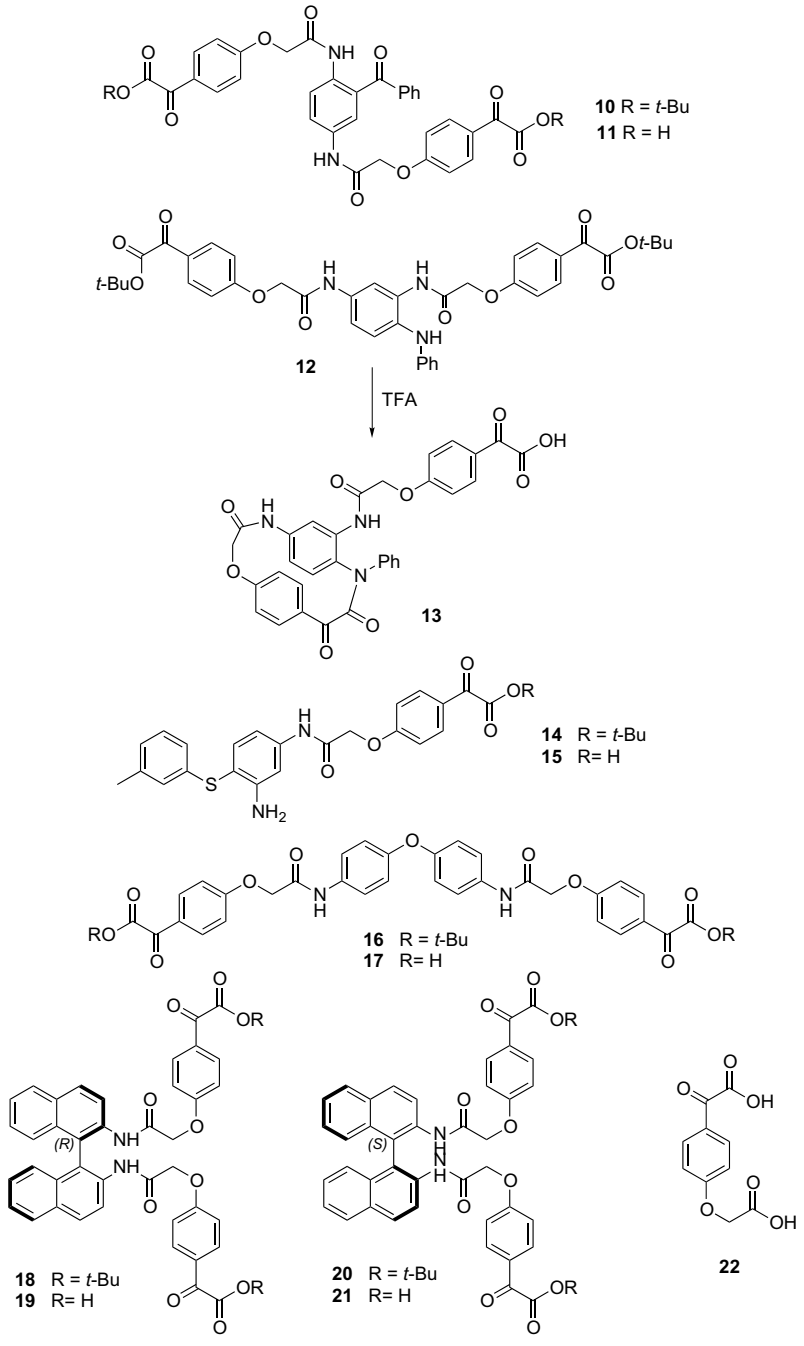

Figure 2. Six best inhibitors, their protected forms and compound **22** (α-ketoacid form of compound **3**).

product. The failure of the second amine to couple with **3** is likely due to steric hindrance caused by the neighboring bulky 3-methylthiophenyl substituent. Several other diamines did not give any detectable coupling product with compound **3**. For example, 9,10-diaminophenanthrene failed in the coupling reaction because it was not soluble in the reaction mixture. 4-Nitro-1,3-phenylenediamine did not couple because the amino groups in this molecule are poor nucleophiles as a result of the strong electron withdrawing character of the nitro substituent.

3. PTPase inhibition studies

The crude inhibitors were screened for activity against the *Yersinia* PTPase, PTP1B, and TCPTP at a concentration of 10 μM (Fig. 3). *para*-Nitrophenyl phosphate

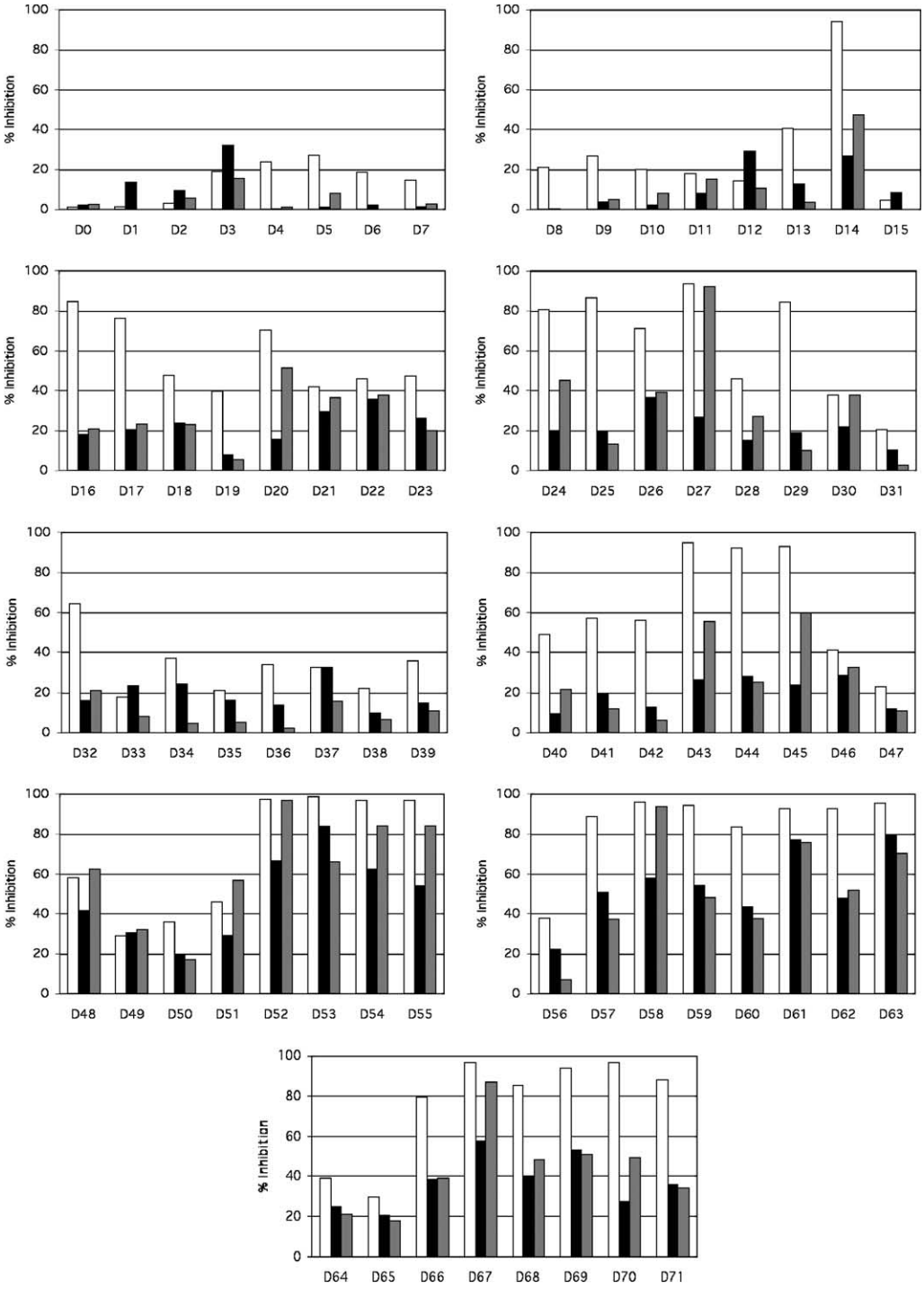

Figure 3. Assay of library members at 10 μM against the *Yersinia* PTPase (open bars), PTP1B (solid bars) and TCPTP (gray bars). Designators on the *x*-axis refer to the library members with the linkages shown in Figure 1. **D0** is the α-ketoacid form of compound **3**, the structure of which is shown in Figure 2 as compound **22**.

was used as the substrate in a 3,3-dimethylglutarate buffer at pH 7.0. Three of the control inhibitors that contained a single α-ketocarboxylic acid unit (**D0**–**D2**) had low activity against all the three enzymes. **D0** corresponds to the diacid that results from deprotection of the *tert*-butyl ester in compound **3**. In contrast, the diester control **D14** had good activity against the *Yersinia* PTPase, and modest activity against PTP1B and TCPTP.

Compounds **D3**–**D12**, which incorporate aliphatic linkers, are all poor inhibitors with less than 30% inhibition at 10 μM against the *Yersinia* PTPase. The remaining compounds (**D13**–**D71**) all contain at least one aromatic ring in the linker structure, and are on average much more active against the PTPases compared to compounds with aliphatic linkers. Several sets of compounds, such as **D10**–**D12**, **D16** and **D17**, and **D70** and **D71**, differ only in the stereochemistry of the linker. Comparison of the activity among these three sets of compounds indicates that the stereochemistry of the linker plays a modest role in controlling the potency of inhibition. It is likely that the inhibitors have enough flexibility to accommodate changes in linker stereochemistry without significantly perturbing the way they bind in the enzyme active site.

Compounds **D20**–**D51** contain a diaminobenzene, diaminopyridine, or diaminopyrimidine linker, and also contain a single aromatic ring. They can be further categorized according to the relative positioning of the two amino groups on the ring. Compounds **D20** and **D23**–**D27** are 1,4-diamines. They have good activity against the *Yersinia* PTPase, but only **D27**, which incorporates a pyridine ring, has significant activity against TCPTP (greater than 90% inhibition at 10 μM). The 1,3-diamines (compounds **D22** and **D28**–**D40**) generally have low activity against all three of the PTPases. Compounds **D29** and **D32** are the only inhibitors out of this group that show higher than 50% inhibition of the *Yersinia* PTPases. Among the 1,2-diamines (compounds **D21** and **D41**–**D51**), **D43**–**D45** are notable for their activity against the *Yersinia* PTPase (greater than 90% inhibition), while **D43**, **D45**, **D48**, and **D51** show moderate activity against TCPTP. None of the compounds that contain a single aromatic ring are good inhibitors of PTP1B.

In contrast to the other compounds, **D52**–**D71** incorporate more than one aromatic ring in the linker structure, and on average are significantly more active than inhibitors with aliphatic linkers or linkers that contain a single aromatic group. All of these compounds, except for **D56**, **D64**, and **D65**, show greater than 80% inhibition of the *Yersinia* PTPase. Among this group, **D52**–**D55**, **D58**, **D61**, **D63**, and **D67** show better than 50% inhibition of both PTP1B and TCPTP at a concentration of 10 μM.

Compound **D52** is a 1,4-diaminobenzene with an added benzoyl substituent. Comparison of **D52** to the other 1,4-diamines (**D20** and **D23**–**D27**) shows that the added benzoyl group improves activity against PTP1B and TCPTP, while maintaining good activity against the *Yersinia* PTPase. Compounds **D53**–**D55** are all 1,3-diaminobenzenes, but they also incorporate an additional aromatic ring. Comparison of their activities to those of the other 1,3-diaminobenzenes (compounds **D22** and **D28**–**D40**) shows that the extra aromatic ring dramatically improves the activities of the inhibitors against all three of the PTPases.

Based upon these initial screening results, we chose to reanalyze the 17 best *Yersinia* PTPase inhibitors at a concentration of 1 μM in order to improve the dynamic range of the assays (Fig. 4). The results show that only inhibitors that incorporate at least two aromatic rings in the linker structure retain significant activity at 1 μM.

We then chose six compounds (Fig. 2) to synthesize on a larger scale and analyze in purified form against the *Yersinia* PTPase, PTP1B, TCPTP, LAR, and CD45. These six compounds correspond to diamines **D52**–**D54**, **D62**, **D70**, and **D71**.

IC_{50} values for the six inhibitors against the five different PTPases are shown in Table 1. All of these compounds are good inhibitors of the *Yersinia* PTPase with IC_{50} values between 5 and 11 μM. They are approximately 15–30-fold more potent than simple monomeric aryl α-ketoacids.[19] This observation is somewhat surprising given that both compounds **13** and **15** incorporate only one α-ketocarboxylic acid group. These data suggest that the additional aromatic components that are present in the linker region of these compounds are partially responsible for enhancing their activity, in addition to the second α-ketocarboxylic acid group. We performed a Lineweaver–Burke analysis of compound **21** using the *Yersinia* PTPase, and demonstrated that it is a reversible competitive inhibitor (Fig. 5). This result is consistent with our previous observations that other inhibitors based on the α-ketoacid motif are also reversible competitive inhibitors of PTPases.[19–22]

The compounds listed in Table 1 are all moderate inhibitors of PTP1B and TCPTP, and show a 1–3-fold selectivity for TCPTP. Since these two PTPases share a 72% sequence identity among the residues that make up the 246 amino acid catalytic domain,[34] it is usually difficult to design inhibitors that show high selectivity for one enzyme over the other. By comparison, the inhibitors show high selectivity against LAR, which is a transmembrane receptor type PTPase that does not

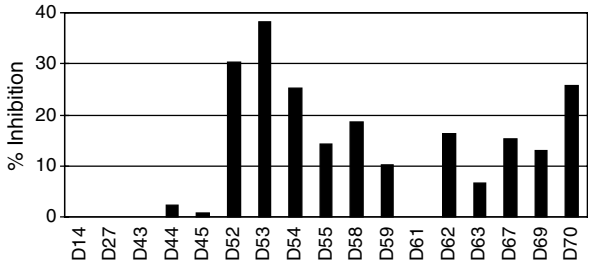

Figure 4. Assay of selected library members at 1 μM against the *Yersinia* PTPase. Designators on the *x*-axis refer to the library members with the linkages shown in Figure 1.

Table 1. Inhibition of phosphatases by compounds **11**, **13**, **15**, **17**, **19**, and **21**[a]

Inhibitor (linker)	IC_{50} (μM)				
	Yersinia PTPase	PTP1B	TCPTP	LAR[b]	CD45
11 (D52)[c]	5.5 ± 0.5	35 ± 7	24 ± 4	0% at 0.5 mM	137 ± 10
13 (D53)	5 ± 1	34 ± 10	10 ± 1	0% at 0.5 mM	260 ± 23
15 (D54)	8.5 ± 1.5	21 ± 2	12.5 ± 1.5	0% at 0.5 mM	75 ± 8
17 (D62)	11 ± 1	102 ± 10	89 ± 5	0% at 0.5 mM	130 ± 23
19 (D70)	11 ± 4	51 ± 5	19 ± 2	0% at 0.5 mM	260 ± 20
21 (D71)	10 ± 3	33 ± 2	14 ± 3	0% at 0.5 mM	120 ± 10

[a] Assays were performed in 50 mM 3,3-dimethylglutarate buffer at pH 7.0, 1 mM EDTA, 50 mM NaCl, and 10% DMSO.
[b] % Inhibition at the given concentration.
[c] Number in the bracket refers to the diamine linker used to generate the inhibitor.

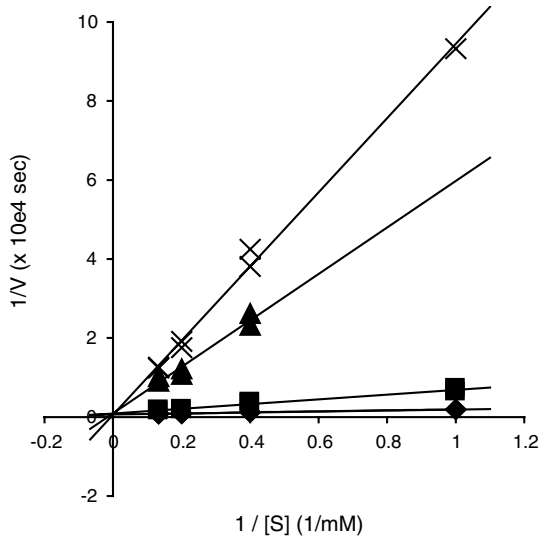

Figure 5. Inhibition of *Yersinia* PTPase by compound **21**. The activity of *Yersinia* PTPase was measured at pH 7.0 as described under the Experimental in the presence of the following concentrations of compound **21**: (♦) 0 μM; (■) 25 μM; (▲) 50 μM; (×) 75 μM. Substrate concentrations used in the assays were 1.0, 2.5, 5.0, and 7.5 mM.

contain the residues that make up the secondary binding site and does not have an Arg in the position that corresponds to Arg-47 of PTP1B. Thus, these residues may play an important role in binding of the inhibitors, and the differences in these regions of the active site may explain the selectivity for the *Yersinia* PTPase, PTP1B, and TCPTP when compared to LAR. Excluding compound **17**, the inhibitors show a 4–8-fold selectivity for PTP1B when compared to CD45. Since CD45 is also a transmembrane receptor type PTPase that lacks the secondary binding site, this observation emphasizes the potential importance of the secondary site in determining the potency of the α-ketocarboxylic acid-based inhibitors. Compounds **19** and **21** differ only in the stereochemistry of the binaphthyl linker. Since the activity of these two compounds is similar for all of the PTPases, the stereochemistry of the linker does not appear to be an important factor in modulating their activity.

The divalent inhibitors may bind in a number of plausible conformations. As we noted earlier, the secondary binding site is not the only target we can utilize to improve the potency and selectivity of inhibitors. For example, Arg-47, Asp-48, and Lys-41 may also contribute to the binding of some of the inhibitors. Simple modeling studies using gOpenMol and Chem3D indicate that the distance between Arg-221 in the active site and Arg-254 in the secondary site is 16.0 Å (based on PDB file 1NNY), while the distance between Arg-221 and Arg-47 is 25.5 Å. The length of compounds **11**, **17**, and **21** are 16.2, 25.0, and 22.0 Å, respectively. Thus, compound **11** can accommodate the distance between the active and secondary sites, while compounds **17** and **21** may be long enough to span the distance between the active site and Arg-47.

4. Conclusions

In summary, we have reported the synthesis and screening of a library of bidentate α-ketocarboxylic acid-based inhibitors. The goal of this study was to examine how the linker region between the two α-ketocarboxylic acids influence the potency of the inhibitors. We have found that aromatic linking groups yield inhibitors that are significantly more active than compounds based upon aliphatic linkers. In addition, the presence of a second aromatic ring in the linker further enhances potency. These results demonstrate that aromatic groups can play an important role in determining binding affinity in this class of inhibitors.

5. Experimental

5.1. General methods

^{1}H NMR and ^{13}C NMR spectra were measured on Bruker Avance-300 or Avance-400 instruments. Chemical shifts were reported relative to TMS ($\delta = 0.00$ ppm) for ^{1}H NMR and $CDCl_3$ ($\delta = 77.0$ ppm) for ^{13}C NMR. Mass spectra were recorded on either a Shimadzu LCMS-QP8000 or an Applied Biosystems QSTAR electrospray mass spectrometer. Solvents were from a Solvent Dispensing System. All reagents were used as received.

5.2. Compound 6

To a suspension of 10 g (73.4 mmol) of 4′-hydroxyacetophenone and 15.2 g (110 mmol) of potassium carbonate in 120 mL DMF, 16.8 g (73.4 mmol) benzyl 2-bromoacetate was added in one portion. The reaction

mixture was stirred at room temperature for 1.5 h. After the solvent was removed by rotary evaporation, the residue was dissolved in 300 mL of 1 N HCl and extracted with EtOAc (2 × 300 mL). The combined organic phases were washed with brine (200 mL) and dried with $MgSO_4$. Filtration and evaporation afforded product **6** as white solid (20.9 g, 100%). The product was used in the next step without further purification. ^{1}H NMR (300 MHz, $CDCl_3$) δ 2.57 (s, 3H), 4.74 (s, 2H), 5.26 (s, 2H), 6.94 (d, J = 8.9 Hz, 2H), 7.35 (m, 5H), 7.93 (d, J = 8.9 Hz, 2H); ^{13}C NMR (75 MHz, $CDCl_3$) δ 26.8, 65.5, 67.6, 114.7, 128.9, 129.1, 131.0, 131.6, 135.4, 161.9, 168.5, 197.1; HRMS-ESI ($M+H^+$) calcd for $C_{17}H_{17}O_4$ 285.1127, found 285.1135.

5.3. Compound 7

Selenium dioxide (7.82 g, 70.4 mmol) was added in one portion to a solution of 10 g (35.2 mmol) of compound **6** dissolved in 300 mL of pyridine. The resulting mixture was heated at reflux for 14 h. After the solvent was removed under reduced pressure, the residue was suspended in 400 mL of 1 N HCl and extracted with EtOAc (2400 mL). The combined organic phases were washed with water (200 mL), brine (200 mL) and dried over $MgSO_4$. Filtration and evaporation afforded product **7** as brown-yellow oil (11 g, 99%). The product was used in the next step without further purification. ^{1}H NMR (300 MHz, $CDCl_3$) 4.79 (s, 2H), 5.27 (s, 2H), 6.99 (d, J = 9.1 Hz, 2H), 7.34 (s, 5H), 8.34 (d, J = 9.1 Hz, 2H), 8.91 (br s, 1H); HRMS-ESI ($M+H^+$) calcd for $C_{17}H_{15}O_6$ 315.0869, found 315.0875.

5.4. Compound 8

A mixture of 10.8 g (34.5 mmol) of **7** and 17.5 mL (103.2 mmol) of thionyl chloride in 120 mL of anhydrous benzene was heated to reflux for 1.5 h. The solvent was removed under reduced pressure. The material was dissolved in 100 mL of anhydrous methylene chloride and the solvent was evaporated to remove excess thionyl chloride. Then 5.1 g (70 mmol) of *tert*-butyl alcohol and 2.7 g (34.5 mmol) of pyridine in 120 mL of anhydrous methylene chloride was added in one portion. The resulting solution was stirred at room temperature overnight. After the solvent was removed under reduced pressure, the residue was purified by chromatography using methylene chloride as the eluent. Compound **8** was obtained as colorless oil (9.01 g, 71%). ^{1}H NMR (300 MHz, $CDCl_3$) δ 1.57 (s, 9H), 4.68 (s, 2H), 5.16 (s, 2H), 6.90 (d, J = 8.8 Hz, 2H), 7.27 (s, 5H), 7.88 (d, J = 8.8 Hz, 2H); ^{13}C NMR (75 MHz, $CDCl_3$) δ 28.4, 65.4, 67.5, 84.9, 115.2, 126.7, 128.8, 129.0 (two overlapping peaks), 132.7, 135.5, 163.2, 164.3, 168.2, 185.7; HRMS-ESI ($M+H^+$) calcd for $C_{21}H_{23}O_6$ 371.1495, found 371.1486.

5.5. Compound 9

A solution of 8.8 g (23.8 mmol) of compound **8** in 100 mL of ethyl acetate was stirred with 1 g of $Pd(OH)_2$ on carbon under an atmosphere of hydrogen gas at room temperature for 24 h. After the starting material had disappeared (as monitored by TLC), the slurry was filtered. The solid was washed with acetone. The organic layers were combined and concentrated to dryness. Recrystallization from acetone yielded compound **9** as white solid (6.2 g, 92%). ^{1}H NMR (300 MHz, MeOH-d_4) δ 1.41 (s, 9H), 4.67 (s, 2H), 5.03 (s, 1H), 5.35 (br s, 2H), 6.95 (d, J = 8.8 Hz, 2H), 7.38 (d, J = 8.7 Hz, 2H); ^{13}C NMR (75 MHz, MeOH-d_4) 27.3, 65.0, 73.2, 82.0, 114.7, 128.2, 132.8, 158.3, 171.7, 172.9; HRMS-ESI ($M+Na^+$) calcd for $C_{14}H_{18}NaO_6$ 305.1001, found 305.0990.

5.6. Compound 3

Dess–Martin Periodinane (1.48 g, 3.48 mmol) was added to a solution of 0.892 g (3.16 mmol) of compound **9** dissolved in 50 mL of acetone. The resulting mixture was stirred at room temperature for 2 h. The mixture was filtered and the solvent was removed under reduced pressure. The residue was dissolved in 50 mL of ether and washed with 50 mL of water and 50 mL of brine. The organic layer was dried over $MgSO_4$ and the solvent evaporated to give 0.82 g (93%) of compound **3** as white solid. ^{1}H NMR (300 MHz, $CDCl_3$) δ 1.61 (s, 9H), 4.80 (s, 2H), 5.08 (br s, 1H), 7.08 (d, J = 8.9 Hz, 2H), 7.91 (d, J = 8.9 Hz, 2H); ^{13}C NMR (75 MHz, $CDCl_3$) δ 27.4, 64.9, 84.9, 115.2, 126.0, 132.3, 163.8, 164.6, 170.6, 186.1; HRMS-ESI ($M+H^+$) calcd for $C_{14}H_{17}O_6$ 281.1025, found 281.1039.

5.7. Synthesis of the library

To a 1 dram vial was added 5 mg (0.018 mmol) of compound **3**, 8 mg of EDC (0.042 mmol), 3 mg of DMAP (0.0246 mmol), 0.009 mmol of the appropriate diamine, and 1 mL of methylene chloride. The reaction was stirred overnight at room temperature and then the solvent was removed by rotary evaporation. The residue was dissolved in 1 mL of EtOAc and washed with 1 N HCl, half-saturated aqueous $NaHCO_3$ solution, and brine. After the solvent was removed, 1 mL of 80% TFA in methylene chloride was added and the solution was stirred for 30 min. The solvent and excess TFA were removed by rotary evaporation to give the final product as a solid.

5.8. Representative procedure for the synthesis of compounds 10–21: Compound 12

To a solution of 100 mg (0.357 mmol) of compound **3**, 140 mg (0.729 mmol) of EDC, and 55 mg (0.451 mmol) of DMAP dissolved in 10 mL of methylene chloride was added 36 mg (0.180 mmol) of diamine **D53**. The reaction was stirred overnight at room temperature. The solvent was then removed and the residue was dissolved in 20 mL of Et_2O. The solution was washed with 20 mL of 1 N HCl and 20 mL of brine. The organic layer was dried over $MgSO_4$ and concentrated to dryness. The residue was purified by flash chromatography (100:2 methylene chloride–Et_2O) to yield compound **12** (98 mg, 0.136 mmol, 76%) as pink powder. ^{1}H NMR (300 MHz, $CDCl_3$) δ 1.63 (s, 18H), 4.60 (s, 2H), 4.68 (s, 2H), 5.59 (br s, 1H), 6.64 (d, J = 7.7 Hz, 2H), 6.75 (d, J = 8.9 Hz,

2H), 6.82 (t, $J = 7.3$ Hz, 1H), 7.08 (d, $J = 8.9$ Hz, 2H), 7.13–7.21 (m, 3H), 7.64 (dd, $J = 8.6$, 2.3 Hz, 1H), 7.81 (d, $J = 8.8$ Hz, 2H), 7.99 (d, $J = 8.8$ Hz, 2H), 8.32 (d, $J = 2.3$ Hz, 1H), 8.41 (s, 1H), 8.88 (s, 1H); ^{13}C NMR (75 MHz, $CDCl_3$) δ 28.5, 67.7, 67.9, 85.1, 85.2, 113.7, 115.2, 115.4, 115.6, 118.2, 120.7, 126.6, 127.3, 127.4, 129.5, 129.9, 132.8, 133.0, 133.3, 134.7, 145.4, 161.9, 162.1, 164.1, 165.7, 166.0, 185.6; HRMS-ESI ($M+Na^+$) calcd for $C_{40}H_{41}N_3NaO_{10}$ 746.2690, found 746.2660.

5.9. Compound 13

Compound **12** (60 mg, 0.083 mmol) was stirred with 5 mL of 80% TFA in methylene chloride for 30 min. The solvent was then removed to afford 45 mg (0.076 mmol, 91%) of compound **13** as gray solid. ^{1}H NMR (300 MHz, $CDCl_3$) δ 4.92 (s, 2H), 5.46 (s, 2H), 7.13–7.27 (m, 5H), 7.53–7.62 (m, 7H), 7.87–7.96 (m, 4H), 8.22 (s, 1H), 10.36 (s, 1H); ^{13}C NMR (75 MHz, $CDCl_3$) δ 63.3, 68.0, 110.1, 111.9, 116.2, 118.8, 126.0, 126.3, 127.5, 130.3, 130.9, 132.8 (two overlapping peaks), 133.0, 135.1, 135.4, 140.4, 149.8, 163.4, 164.1, 166.6, 167.2, 167.3, 187.9, 188.0; HRMS-ESI ($M-H^-$) calcd for $C_{32}H_{22}N_3O_9$ 592.1356, found 592.1335.

5.10. Compound 10

Compound **10** was prepared from compound **3** and diamine **D52** by procedures analogous to the preparation of compound **12** (dark red powder, 73 mg, 0.099 mmol, 56%). ^{1}H NMR (300 MHz, $CDCl_3$) δ 1.62 (s, 18H), 4.65 (s, 2H), 4.70 (s, 2H), 7.04 (d, $J = 8.5$ Hz, 2H), 7.18 (d, $J = 8.7$ Hz, 2H), 7.50 (t, $J = 7.4$ Hz, 2H), 7.61 (t, $J = 7.2$ Hz, 1H), 7.70 (d, $J = 8.6$ Hz, 1H), 7.77 (d, $J = 7.3$ Hz, 2H), 7.97 (m, 5H), 8.40 (s, 1H), 8.68 (d, $J = 8.9$ Hz, 1H), 11.6 (s, 1H); ^{13}C NMR (75 MHz, $CDCl_3$) δ 28.5, 67.7 (two overlapping peaks), 85.1, 85.3, 115.4, 115.5, 122.6, 124.9, 125.6, 126.2, 127.2, 127.4, 128.8, 130.5, 132.1, 132.9, 133.0, 133.4, 136.2, 138.3, 162.0, 162.3, 164.0, 164.2, 165.8, 166.6, 185.6, 185.8, 198.7; HRMS-ESI ($M+Na^+$) calcd for $C_{41}H_{40}N_2NaO_{11}$ 759.2530, found 759.2520.

5.11. Compound 11

Compound **11** was prepared from 73 mg of compound **10** by procedures analogous to the preparation of compound **13** (gray powder, 60 mg, 0.096 mmol, 97%). ^{1}H NMR (300 MHz, DMSO-d_6) δ 4.70 (s, 2H), 4.85 (s, 2H), 7.16 (dd, $J = 9.4$ Hz, 4H), 7.52 (t, $J = 7.5$ Hz, 2H), 7.65 (t, $J = 7.2$ Hz, 1H), 7.72 (d, $J = 7.3$ Hz, 2H), 7.80 (d, $J = 1.9$ Hz, 1H), 7.89–7.96 (m, 6H), 10.4 (s, 1H), 10.7 (s, 1H); ^{13}C NMR (75 MHz, DMSO-d_6) δ 67.8, 116.2 (two overlapping peaks), 122.8, 124.4, 124.6, 126.0, 126.2, 129.3, 129.8, 130.6, 132.8, 133.0, 133.7, 135.3, 138.0, 163.4, 164.0, 166.8, 167.2, 167.3, 187.9, 196.9; HRMS-ESI ($M-H^-$) calcd for $C_{33}H_{23}N_2O_{11}$ 623.1302, found 623.1325.

5.12. Compound 14

Compound **14** was prepared from compound **3** and 41 mg of diamine **D54** by procedures analogous to the preparation of compound **12** (pink solid, 55 mg, 0.112 mmol, 63%). ^{1}H NMR (300 MHz, $CDCl_3$) δ 1.64 (s, 9H), 2.27 (s, 3H), 4.31 (br s, 2H), 4.69 (s, 2H), 6.76–6.94 (m, 4H), 7.06–7.13 (m, 3H), 7.37–7.43 (m, 2H), 8.02 (d, $J = 8.9$ Hz, 2H), 8.20 (s, 1H); ^{13}C NMR (75 MHz, $CDCl_3$) δ 21.8, 28.5, 67.9, 85.2, 106.6, 110.5, 110.9, 115.4, 123.8, 126.8, 127.3, 127.6, 129.3, 133.0, 137.0, 138.6, 139.3, 139.6, 150.2, 162.0, 164.0, 165.6, 185.6; HRMS-ESI ($M-H^-$) calcd for $C_{27}H_{27}N_2O_5S$ 491.1641, found 491.1630.

5.13. Compound 15

Compound **15** was prepared from 55 mg of compound **14** by procedures analogous to the preparation of compound **13** (gray powder, 48 mg, 0.11 mmol, 98%). ^{1}H NMR (300 MHz, DMSO-d_6) δ 2.21 (s, 3H), 4.87 (s, 2H), 6.79–6.94 (m, 4H), 7.11–7.27 (m, 5H), 7.93 (d, $J = 8.8$ Hz, 2H), 10.1 (s, 1H); ^{13}C NMR (75 MHz, DMSO-d_6) δ 21.8, 67.9, 106.1, 107.6, 109.5, 116.2, 123.9, 125.9, 126.9, 127.2, 129.7, 132.8, 137.9, 138.5, 139.1, 141.8, 151.5, 164.1, 166.6, 167.3, 188.0; HRMS-ESI ($M-H^-$) calcd for $C_{23}H_{19}N_2O_5S$ 435.1015, found 435.1025.

5.14. Compound 16

Compound **16** was prepared from compound **3** and 36 mg of diamine **D62** by procedures analogous to the preparation of compound **12** (white solid, 66 mg, 0.091 mmol, 51%). ^{1}H NMR (300 MHz, $CDCl_3$) δ 1.62 (s, 18H), 4.68 (s, 4H), 6.98 (d, $J = 8.6$ Hz, 4H), 7.06 (d, $J = 8.5$ Hz, 4H), 7.55 (d, $J = 8.7$ Hz, 4H), 7.98 (d, $J = 8.5$ Hz, 4H), 8.34 (s, 2H); ^{13}C NMR (75 MHz, $CDCl_3$) δ 28.5, 67.8, 85.3, 115.4, 119.7, 122.6, 127.4, 132.5, 133.0, 154.6, 162.2, 164.1, 165.6, 185.7; HRMS-ESI ($M+Na^+$) calcd for $C_{40}H_{40}N_2NaO_{11}$ 747.2530, found 747.2534.

5.15. Compound 17

Compound **17** was prepared from 66 mg of compound **16** by procedures analogous to the preparation of compound **13** (white solid, 52 mg, 0.085 mmol, 93%). ^{1}H NMR (300 MHz, DMSO-d_6) δ 4.87 (s, 4H), 6.98 (d, $J = 8.9$ Hz, 4H), 7.20 (d, $J = 8.8$ Hz, 4H), 7.62 (d, $J = 8.9$ Hz, 4H), 7.94 (d, $J = 8.8$ Hz, 4H), 10.2 (s, 2H); ^{13}C NMR (75 MHz, DMSO-d_6) δ 67.8, 116.2, 119.6, 122.3, 126.0, 132.8, 134.7, 153.7, 164.0, 166.4, 167.3, 188.0; HRMS-ESI ($M-H^-$) calcd for $C_{32}H_{23}N_2O_{11}$ 611.1302, found 611.1310.

5.16. Compound 18

Compound **18** was prepared from compound **3** and 50 mg of diamine **D70** by procedures analogous to the preparation of compound **12** (brown powder, 72 mg, 0.089 mmol, 50%). ^{1}H NMR (300 MHz, $CDCl_3$) δ 1.66 (s, 18H), 4.40 (dd, $J = 22.7$, 15.1 Hz, 4H), 6.32 (d, $J = 8.9$ Hz, 4H), 7.02 (d, $J = 8.4$ Hz, 2H), 7.24 (t, $J = 7.6$ Hz, 2H), 7.44 (t, $J = 7.5$ Hz, 2H), 7.76 (d, $J = 8.9$ Hz, 4H), 7.93 (d, $J = 8.1$ Hz, 2H), 8.02 (s, 2H), 8.08 (d, $J = 9.1$ Hz, 2H), 8.70 (d, $J = 9.0$ Hz, 2H); ^{13}C

NMR (100 MHz, $CDCl_3$) δ 28.5, 67.5, 85.1, 114.6, 120.0, 120.6, 125.1, 126.4, 127.2, 128.2, 128.9, 130.8, 131.7, 132.5, 132.7, 134.3, 161.4, 164.1, 165.8, 185.5; HRMS-ESI ($M-H^-$) calcd for $C_{48}H_{43}N_2O_{10}$ 807.2918, found 807.2895.

5.17. Compound 19

Compound **19** was prepared from 55 mg of compound **18** by procedures analogous to the preparation of compound **13** (dark brown powder, 61 mg, 0.088 mmol, 98%). ^1H NMR (300 MHz, acetonitrile-d_3) δ 4.43 (dd, $J = 18.2$, 15.4 Hz, 4H), 5.86 (br s, 2H), 6.46 (d, $J = 9.0$ Hz, 4H), 6.94 (d, $J = 8.5$ Hz, 2H), 7.24 (m, 2H), 7.44 (m, 2H), 7.85 (d, $J = 9.0$ Hz, 4H), 7.98 (d, $J = 8.1$ Hz, 2H), 8.12 (d, $J = 9.0$ Hz, 2H), 8.27 (s, 2H), 8.38 (d, $J = 9.0$ Hz, 2H); ^{13}C NMR (75 MHz, acetonitrile-d_3) δ 67.4, 114.8, 122.0, 122.8, 125.0, 126.3, 126.4, 127.8, 128.9, 130.4, 131.9, 132.6, 132.9, 134.5, 162.2, 164.5, 166.9, 185.5; HRMS-ESI ($M-H^-$) calcd for $C_{40}H_{27}N_2O_{10}$ 695.1666, found 695.1650.

5.18. Compound 20

Compound **20** was prepared from compound **3** and 50 mg of diamine **D71** by procedures analogous to the preparation of compound **20** (brown powder, 68 mg, 0.084 mmol, 47%). ^1H NMR (300 MHz, $CDCl_3$) δ 1.66 (s, 18H), 4.40 (dd, $J = 22.7$, 15.2 Hz, 4H), 6.32 (d, $J = 8.8$ Hz, 4H), 7.02 (d, $J = 8.4$ Hz, 2H), 7.24 (t, $J = 7.6$ Hz, 2H), 7.44 (t, $J = 7.2$ Hz, 2H), 7.76 (d, $J = 8.8$ Hz, 4H), 7.93 (d, $J = 8.2$ Hz, 2H), 8.01 (s, 2H), 8.08 (d, $J = 9.1$ Hz, 2H), 8.70 (d, $J = 9.0$ Hz, 2H); ^{13}C NMR (75 MHz, $CDCl_3$) δ 28.5, 67.5, 85.1, 114.6, 120.0, 120.6, 125.1, 126.4, 127.2, 128.2, 128.9, 130.8, 131.7, 132.5, 132.7, 134.3, 161.4, 164.1, 165.8, 185.5; HRMS-ESI ($M-H^-$) calcd for $C_{48}H_{45}N_2O_{10}$ 809.3074, found 809.3055.

5.19. Compound 21

Compound **21** was prepared from 55 mg of compound **20** by procedures analogous to the preparation of compound **13** (dark brown powder, 55 mg, 0.079 mmol, 94%). ^1H NMR (300 MHz, acetonitrile-d_3) δ 4.44 (dd, $J = 18.2$, 15.4 Hz, 4H), 6.44 (d, $J = 8.9$ Hz, 4H), 6.94 (d, $J = 8.5$ Hz, 2H), 7.22 (m, 2H), 7.43 (m, 2H), 7.84 (d, $J = 8.9$ Hz, 4H), 7.96 (d, $J = 8.1$ Hz, 2H), 8.10 (d, $J = 8.9$ Hz, 2H), 8.32 (d, $J = 9.0$ Hz, 2H), 8.37 (s, 2H), 8.90 (br s, 2H); ^{13}C NMR (75 MHz, acetonitrile-d_3) δ 67.4, 114.9, 122.1, 123.1, 125.0, 126.3, 126.5, 127.8, 128.9, 130.4, 132.0, 132.6, 132.9, 134.4, 162.2, 164.3, 167.2, 185.3; HRMS-ESI ($M-H^-$) calcd for $C_{40}H_{27}N_2O_{10}$ 695.1666, found 695.1661.

5.20. PTPase assays

The phosphatase activities of the *Yersinia* PTPase, PTP1B, LAR, TCPTP, and CD45 were assayed using *p*-NPP as the substrate at room temperature and the reaction progress was monitored by UV spectroscopy. Initial rates were determined by monitoring the hydrolysis of *p*-NPP at 405 nm, from 10 to 130 s after mixing. Assay solutions contained 50 mM 3,3-dimethylglutarate at pH 7.0, 1 mM EDTA, 50 mM NaCl, and 10% DMSO. For percent inhibition assays, the substrate concentrations were kept at 2.9, 2.0, and 2.0 mM for *Yersinia* PTPase, PTP1B, and TCPTP assays, respectively. For IC_{50} assays, the substrate concentrations were kept at the K_m value. The K_m values in this buffer were found to be 2.9, 2.0, 2.3, 2.1, and 7.0 mM for the *Yersinia* PTPase, PTP1B, LAR, TCPTP, and CD45, respectively. IC_{50} values were calculated using a Dixon analysis. Data analysis was performed with the commercial graphing package Grafit (Erithacus Software Ltd).

5.21. Molecular modeling

The geometry of inhibitors was optimized using MOPAC in Chem3D to afford a minimum energy conformation. The distances between residues in PTP1B (structure 1NNY in the Protein Data Bank) were calculated using gOpenMol (available at http://www.csc.fi/gopenmol/). The lengths of the inhibitors were defined as the distance between the two carbonyl oxygen atoms in the two α-keto acid groups of each inhibitor as calculated by gOpenMol.

Acknowledgements

This research was supported by the NIH NIGMS (R01 GM057327).

Supplementary data

^1H and ^{13}C NMR spectra for compounds **3** and **6**–**21** are available as supplementary data from ScienceDirect at http://www.sciencedirect.com. Supplementary data associated with this article can be found, in the online version, at doi:10.1016/j.bmc.2005.02.001.

References and notes

1. Zhang, Z. Y. *Acc. Chem. Res.* **2003**, *36*, 385.
2. Blaskovich, M. A.; Kim, H. O. *Exp. Opin. Ther. Pat.* **2002**, *12*, 871.
3. Elchebly, M.; Payette, P.; Michaliszyn, E.; Cromlish, W.; Collins, S.; Loy, A. L.; Normandin, D.; Cheng, A.; Himms-Hagen, J.; Chan, C.-C.; Ramachandran, C.; Gresser, M. J.; Tremblay, M. L.; Kennedy, B. P. *Science* **1999**, *283*, 1544.
4. Klaman, L. D.; Boss, O.; Peroni, O. D.; Kim, J. K.; Martino, J. L.; Zabolotny, J. M.; Moghal, N.; Lubkin, M.; Kim, Y.-B.; Sharpe, A. H.; Stricker-Krongrad, A.; Shulman, G. I.; Neel, B. G.; Kahn, B. B. *Mol. Cell. Biol.* **2000**, *20*, 5479.
5. YouTen, K. E.; Muise, E. S.; Itie, A.; Michaliszyn, E.; Wagner, J.; Jothy, S.; Lapp, W. S.; Tremblay, M. L. *J. Exp. Med.* **1997**, *186*, 683.
6. Ibarra-Sanchez, M.; Tremblay, M.; Simoncic, P. Patent WO 00/36111.
7. Schaapveld, R. Q. J.; Schepens, H. T. G.; Robinson, G. W.; Attema, J.; Oerlemans, F. T. J. J.; Fransen, J. A. M.; Streuli, M.; Wieringa, B.; Hennighausen, L.; Hendriks, W. J. A. J. *Dev. Biol.* **1997**, *188*, 134.

8. Yeo, T. T.; Yang, T.; Massa, S. M.; Zhang, J. S.; Honkaniemi, J.; Butcher, L. L.; Longo, F. M. *J. Neurosci. Res.* **1997**, *47*, 348.
9. Ren, J. M.; Li, P. M.; Zhang, W. R.; Sweet, L. J.; Cline, G.; Shulman, G. I.; Livingston, J. N.; Goldstein, B. J. *Diabetes* **1998**, *47*, 493.
10. Muller, T.; Ullrich, A. Patent WO 00/61180.
11. Thomas, M. L.; Brown, E. J. *Immunol. Today* **1999**, *20*, 406.
12. Kung, C.; Pingel, J. T.; Heikinheimo, M.; Klemola, T.; Varkila, K.; Yoo, L. I.; Vuopala, K.; Poyhonen, M.; Uhari, M.; Rogers, M.; Speck, S. H.; Chatila, T.; Thomas, M. L. *Nat. Med.* **2000**, *6*, 343.
13. Urbanek, R. A.; Suchard, S. J.; Steelman, G. B.; Knappenberger, K. S.; Sygowski, L. A.; Veale, C. A.; Chapdelaine, M. J. *J. Med. Chem.* **2001**, *44*, 1777.
14. Lazarovits, A. I.; Poppema, S.; Zhang, Z.; Khandaker, M.; LeFeuvre, C. E.; Singhal, S. K.; Garcia, B. M.; Ogasa, N.; Jevnikar, A. M.; White, M. J.; Singh, G.; Stiller, C. R.; Zhong, R. Z. *Nature* **1996**, *380*, 717.
15. Bliska, J. B.; Guan, K. L.; Dixon, J. E.; Falkow, S. *Proc. Natl. Acad. Sci. U.S.A.* **1991**, *88*, 1187.
16. Leung, C.; Grzyb, J.; Lee, J.; Meyer, N.; Hum, G.; Jia, C. G.; Liu, S. F.; Taylor, S. D. *Bioorg. Med. Chem.* **2002**, *10*, 2309.
17. Larsen, S. D.; Stevens, F. C.; Lindberg, T. J.; Bodnar, P. M.; O'Sullivan, T. J.; Schostarez, H. J.; Palazuk, B. J.; Bleasdale, J. E. *Bioorg. Med. Chem. Lett.* **2003**, *13*, 971.
18. Xie, J.; Comeau, A. B.; Seto, C. T. *Org. Lett.* **2004**, *6*, 83.
19. Chen, Y. T.; Onaran, M. B.; Doss, C. J.; Seto, C. T. *Bioorg. Med. Chem. Lett.* **2001**, *11*, 1935.
20. Chen, Y. T.; Seto, C. T. *J. Med. Chem.* **2002**, *45*, 3946.
21. Chen, Y. T.; Xie, J.; Seto, C. T. *J. Org. Chem.* **2003**, *68*, 4123.
22. Chen, Y. T.; Seto, C. T. *Bioorg. Med. Chem.* **2004**, *12*, 3289.
23. Zhang, Z. Y.; Wang, Y.; Wu, L.; Fauman, E. B.; Stuckey, J. A.; Schubert, H. L.; Saper, M. A.; Dixon, J. E. *Biochemistry* **1994**, *33*, 15266.
24. Puius, Y. A.; Zhao, Y.; Sullivan, M.; Lawrence, D. S.; Almo, S. C.; Zhang, Z. Y. *Proc. Natl. Acad. Sci. U.S.A.* **1997**, *94*, 13420.
25. Szczepankiewicz, B. G.; Liu, G.; Hajduk, P. J.; Abad-Zapatero, C.; Pei, Z. H.; Xin, Z. L.; Lubben, T. H.; Trevillyan, J. M.; Stashko, M. A.; Ballaron, S. J.; Liang, H.; Huang, F.; Hutchins, C. W.; Fesik, S. W.; Jirousek, M. R. *J. Am. Chem. Soc.* **2003**, *125*, 4087.
26. Taing, M.; Keng, Y. F.; Shen, K.; Wu, L.; Lawrence, D. S.; Zhang, Z. Y. *Biochemistry* **1999**, *38*, 3793.
27. Shen, K.; Keng, Y. F.; Wu, L.; Guo, X. L.; Lawrence, D. S.; Zhang, Z. Y. *J. Biol. Chem.* **2001**, *276*, 47311.
28. Jia, Z. C.; Ye, Q. L.; Dinaut, A. N.; Wang, Q. P.; Waddleton, D.; Payette, P.; Ramachandran, C.; Kennedy, B.; Hum, G.; Taylor, S. D. *J. Med. Chem.* **2001**, *44*, 4584.
29. Guo, X. L.; Kui, S.; Wang, F.; Lawrence, D. S.; Zhang, Z. Y. *J. Biol. Chem.* **2002**, *277*, 41014.
30. Sun, J. P.; Fedorov, A. A.; Lee, S. Y.; Guo, X. L.; Shen, K.; Lawrence, D. S.; Almo, S. C.; Zhang, Z. Y. *J. Biol. Chem.* **2003**, *278*, 12406.
31. Asante-Appiah, E.; Patel, S.; Dufresne, C.; Roy, P.; Wang, Q. P.; Patel, V.; Friesen, R. W.; Ramachandran, C.; Becker, J. W.; Leblanc, Y.; Kennedy, B. P.; Scapin, G. *Biochemistry* **2002**, *41*, 9043.
32. Ethyl bromoacetate was used to introduce the carboxylic acid functionality for coupling with diamines. However, due to the instability of α-ketoacid *tert*-butyl ester under basic conditions, selective deprotection of the ethyl ester in the presence of the *tert*-butyl ester was not successful.
33. Eickhoff, D.; Degenhardt, C.; Mciver, J. Patent WO 00/18733.
34. Galic, S.; Klingler-Hoffmann, M.; Fodero-Tavoletti, M. T.; Puryer, M. A.; Meng, T. C.; Tonks, N. K.; Tiganis, T. *Mol. Cell. Biol.* **2003**, *23*, 2096.